



Uncatalyzed gas phase aziridination of alkenes by organic azides. Part 2. Whole azide reaction with alkene

S PREMILA DEVI and R H DUNCAN LYNGDOH*

Department of Chemistry, North-Eastern Hill University, Shillong, Meghalaya 793 022, India
E-mail: rhdl@nehu.ac.in

MS received 13 September 2018; revised 17 October 2018; accepted 20 October 2018; published online 4 January 2019

Abstract. The B3LYP/6-31G(d,p) DFT method was used to study alkene aziridination by azides through uncatalyzed thermal gas phase routes which involve the whole azide reactant molecule without dissociation. Two mechanisms were studied – Route I involving concerted azide addition to alkene with the elimination of N_2 , and the multi-step Route II involving 1,3-dipolar cycloaddition between azide and alkene. Three azides RN_3 ($R = H, Me, Ac$) are reacted with alkene substrates forming aziridine products. The concerted addition–elimination step of Route I is exothermic with an appreciable barrier, where the facility order $Ac > Me > H$ points to electrophilicity of the azide reactant. The initial 1,3-dipolar cycloaddition step of Route II involves smaller barriers than Route I, while thermal decomposition of the triazoline intermediate to aziridine and N_2 involves two more steps with an N-alkylimine intermediate. The very high barrier for N-alkylimine cyclization to aziridine could be offset by the high exothermicity of the previous step. Geometries of the transition states for various reaction steps studied here are described as ‘early’ or ‘late’ in good accordance with the Hammond postulate. Two other mechanisms (Routes A and B) studied earlier (involving discrete nitrene intermediates) are compared with Routes I and II, where Route II involving 1,3-dipolar cycloaddition is predicted to be energetically the most favored of all the four mechanisms for thermal gas-phase aziridination of alkenes by azides.

Keywords. Alkene aziridination by azides; 1,3-dipolar cycloaddition; triazoline decomposition; density functional theory.

1. Introduction

Nitrene addition to a C=C double bond is one strategy for aziridine synthesis,^{1,2} using substrates including alkenes and fullerenes.^{3,4} Azides are prominent as carriers of the nitrene moiety, which may be written as $-NR$ or $:NR$ for the free nitrene.^{5,6} A noteworthy aspect of aziridine synthesis is asymmetric aziridination^{7,8} which includes a variety of substrates, reagents and catalysts.^{9–14} This paper, however, considers only the bare, thermal, uncatalyzed aziridination reaction in the gas phase. In this context, whether alkene aziridination involves nitrenes as a discrete species or as a transferred moiety is a question of interest. An earlier computational study¹⁵ considered the possibility of free nitrene species participating in this reaction. The present study treats the whole (undissociated) azide molecules as nitrene transfer agents for alkene aziridination.

1.1 Mechanisms for alkene aziridination by azides

Two mechanisms for alkene aziridination by whole azide molecules are considered here. Route I, proposed for the first time, involves the concerted addition of azide to alkene with the elimination of N_2 . Route II involves the well-known 1,3-dipolar cycloaddition of azide to alkene, followed by decomposition of the triazoline intermediate to the aziridine releasing N_2 . Which route is more feasible is predicted here computationally, and then compared with the two earlier routes¹⁵ involving the participation of discrete nitrene species.

Three azide reactants are considered here – hydrazoic acid HN_3 , methyl azide MeN_3 and acetyl azide AcN_3 (Figure 1) – in order to examine the effects of change in the R group of the azide RN_3 . The nitrene moiety transferred during aziridination is $RN-$ ($R = H, Me$ and Ac). Four alkene substrates ethene, propene,

*For correspondence

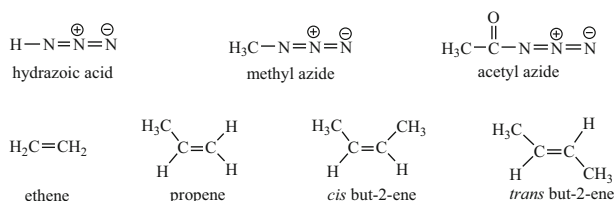


Figure 1. Azides as nitrene transfer agents and alkenes as substrates for aziridination.

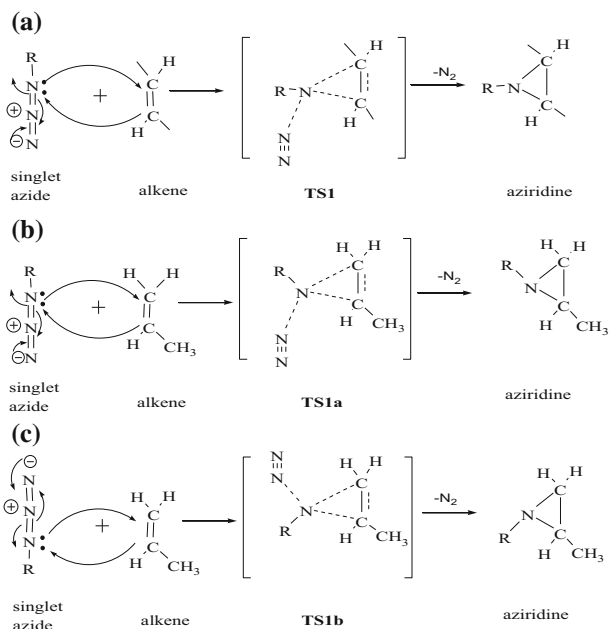


Figure 2. Mechanisms for (a) concerted addition–elimination aziridination of alkene (*trans*-2-butene as an example) by azide, along with (b) propene A case, and (c) propene B case.

cis- and *trans*-2-butene (Figure 1) are chosen to study the effects of successive methyl substitution.

Route I (Figure 2) is concerted, where the **R**–N moiety of the azide attacks the alkene C=C bond with loss of N₂, proceeding *via* transition state **TS1**. For ethene, *cis*- and *trans*-2-butene, there is only one energetically unique orientation for the approach of the azide to the alkene. For the asymmetrical propene case, there are two orientations (Figures 2b and 2c), with the azide **R** group pointing away from and towards the propene methyl group, proceeding through transition states **TS1a** and **TS1b** respectively (the propene A and propene B cases).

Route II has two phases. The first phase (Figure 3) is concerted 1,3-dipolar cycloaddition of singlet azide to the alkene. This thermal pericyclic reaction proceeds *via* transition state **TS2** to yield the 1,2,3-triazoline intermediate. The asymmetrical propene gives two orientations (propene A and propene B) shown in Figures 3b and 3c, where the azide **R** group points towards and away from

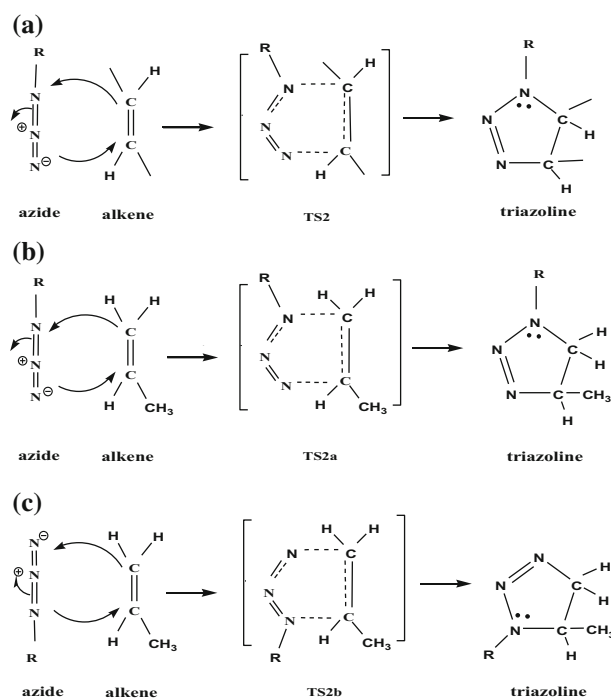


Figure 3. First phase of Route II: 1,3-dipolar cycloaddition of azide to alkene (*trans*-2-butene as an example), showing also (b) propene A case, and (c) propene B case.

the methyl group, proceeding *via* transition states **TS2a** and **TS2b**.

1,3-Dipolar cycloaddition (the first step of Route II) has wide synthetic utility.^{16,17} The Huisgen 1,3-dipolar cycloaddition¹⁸ between azides and alkynes yields 1,2,3-triazole products, well-known as a metal-catalyzed reaction.¹⁹ This reaction is of much importance for click chemistry,²⁰ and has been employed to enable live cell imaging.²¹ However, such a reaction between azides and *alkenes* has not been studied as much and is mentioned here for its relevance to aziridine synthesis.

In the second phase of Route II (Figure 4), the intermediate formed in the first phase undergoes 1,2-hydride shift to yield an acyclic intermediate with loss of N₂ *via* transition state **TS3**. Subsequent ring closure through 1,2-hydride shift leads to the aziridine product *via* transition state **TS4**. For the first step of this second phase, the propene case may have the **R** group pointing towards and away from the propene methyl group, proceeding *via* transition states **TS3a** and **TS3b** respectively (Figures 4b and 4c). The two N-alkylimine products formed rearrange to give two different final aziridine products *via* the transition states **TS4a** and **TS4b** respectively. These two aziridines may interconvert *via* inversion at the N-atom, but this may involve a barrier not easily overcome at room temperature.

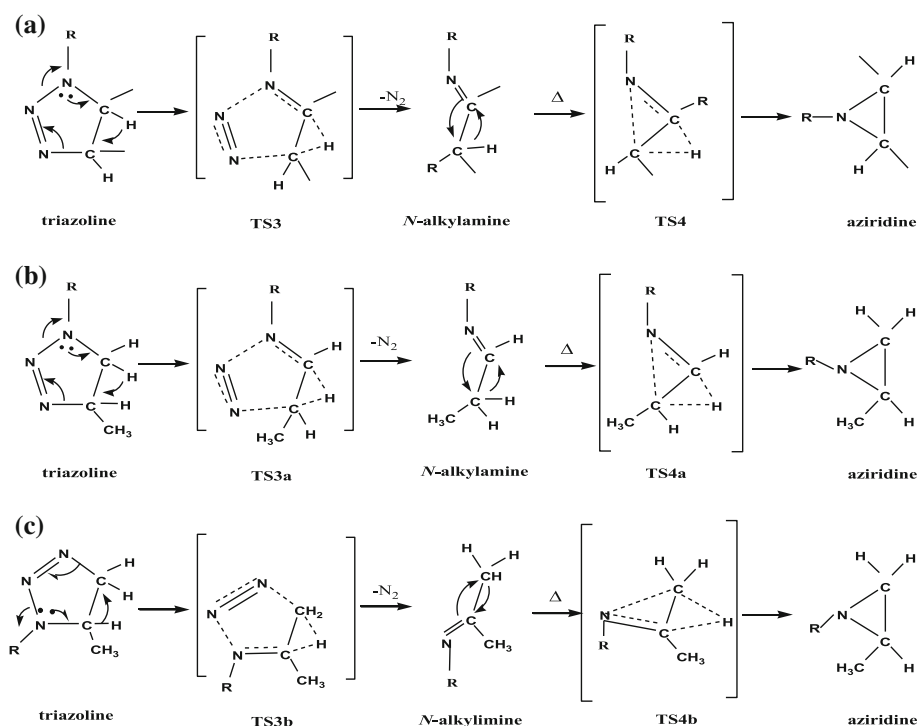


Figure 4. Second phase of Route II – the two-step decomposition of 1,2,3-triazoline to aziridine and N_2 via an N-alkylimine intermediate, along with (b) the propene A case, and (c) the propene B case.

1.2 1,3-Dipolar cycloadditions with azides

A CBS-QB3 study on cycloadditions of alkenes and ynamines with 1,3-dipoles yielded trends in activation barrier values and regioselectivity.^{22,23} A B3LYP and SCS-MP2 study on regioselectivity of cycloadditions of azides to cyclic alkynes and alkenes²⁴ treated the effects of fluorine substitution, strain, ring size and multiple bond type. Such effects in metal-free azide-alkyne click reactions were studied in the context of biological processes.²⁵ A B3LYP study described substituent effects on transition states for the aziridination of various alkenes by oxaziridines and diaziridinium salts.²⁶ Cycloaddition of benzyl azide to acrylic acid was studied by the B3LYP method.²⁷ Strain energies and hydrogenation enthalpies for cyclic alkynes and alkenes, computed by the G3 method, were correlated with activation barriers for cycloaddition between various azides and these substrates.²⁸ A DFT-cum-experimental study on reactions between aryl azides and activated alkenes²⁹ rationalized regioselectivity trends. 1,3-Dipolar cycloaddition of methyl azide to C_{60} with stepwise N_2 elimination from the intermediate to yield the aziridine was studied using the AM1 and DFT methods.³⁰

Aziridination of aldimines by sulfur ylides was studied by DFT to study substituent effects upon

diastereoselectivity.³¹ A DFT study on aziridine formation from guanidinium ylide and p-substituted benzaldehydes predicted substituent effects upon diastereoselectivity.³² Mechanistic studies using DFT on aziridination with arsenic ylides identified the roles of steric and electrostatic interactions for diastereoselectivity.³³ Mechanisms of ring opening for aziridines and for boriranes have been compared using ab initio and DFT approaches.³⁴

1.3 Scope and objectives of the study

In this study, the undissociated azide molecule as a whole acts as the aziridinating agent, not the free nitrene as studied earlier.¹⁵ Three azides $R-N_3$ are taken as nitrene transfer agents [$R = H, Me$ and Ac (acetyl)] and four alkenes (ethene, propene, *cis*- and *trans*-2-butene) as substrates (Figure 1). Two routes are considered here, *viz.*, (a) concerted addition–elimination of the azide $R-N_3$, called Route I, and (b) a two-phase pathway involving 1,3-dipolar cycloaddition and decomposition of a triazoline intermediate, called Route II. The aims of this study are as follows:

1. To discern the effects of (a) change in the R group of the azide reactant RN_3 and (b) methyl substitution in the alkene substrates for aziridination facility. For each

concerted step, the activation barrier and accompanying energy change represent are used to indicate facility.

2. To correlate transition state geometry with reaction energetics as per the Hammond postulate for the various one-step reactions studied here.

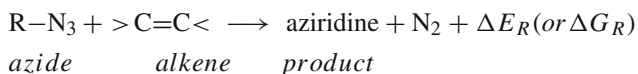
3. To predict the most feasible of the four distinct routes for alkene aziridination by azides, *viz.*, Routes I and II, along with two other mechanisms studied earlier involving discrete nitrene intermediates.¹⁵

2. Computational methods and strategy

The B3LYP DFT method^{35,36} with a 6-31G** basis set was used to study the two routes proposed above. Vibrational frequency analysis characterized all species either as energy minima or transition states. Zero point vibrational energies (ZPE) were corrected by a scaling factor of 0.9806 prescribed for the B3LYP/6-31G(d,p) strategy.³⁷ All computations were carried out using the Gaussian 2009 program.³⁸

Transition states were located by interpolation between reactant and product geometries. For steps with two reactants, an entry complex was set up keeping a constant non-bonded distance between the appropriate atoms and optimizing other internal coordinates. Likewise, steps yielding two products were treated by setting up an initial exit complex.

Energetics were monitored by estimating the energy change for any one step (denoted as ΔE_r or ΔG_r for the enthalpy or free energy change respectively), and also the activation barrier (denoted as ΔE^\ddagger and ΔG^\ddagger in enthalpy and free energy terms respectively). The net reaction given below for aziridination of alkene by azide is associated with the net enthalpy change ΔE_R (or net free energy change ΔG_R), independent of the mechanism.



For both Route I and Route II, an energy profile is plotted setting the energy level of the initial reactants as zero and including all stages along the pathway. This was also done for the two routes of the earlier DFT study¹⁵ which involved discrete nitrene species. This is done to predict the energetically most feasible option among the four mechanisms proposed.

Transition state geometries are examined for the effects of the azide **R** groups and alkene substituents, and to relate transition state geometry to the Hammond postulate.³⁹ This states that for reactions with a modest barrier, exothermic reactions proceed *via* 'early' transition states which resemble the reactants in geometry and energy. Endothermic reactions have 'late' transition states which resemble the products.

Figure 5 depicts select geometry parameters for the transition states (a) **TS1** for concerted addition–elimination of azide to alkene (Route I), (b) **TS2** for 1,3-dipolar cycloaddition between azide and alkene (first phase of Route II), (c) **TS3** for 1,2-hydride shift in triazoline to form N-alkylimine intermediate (initial step of second phase of Route II), and

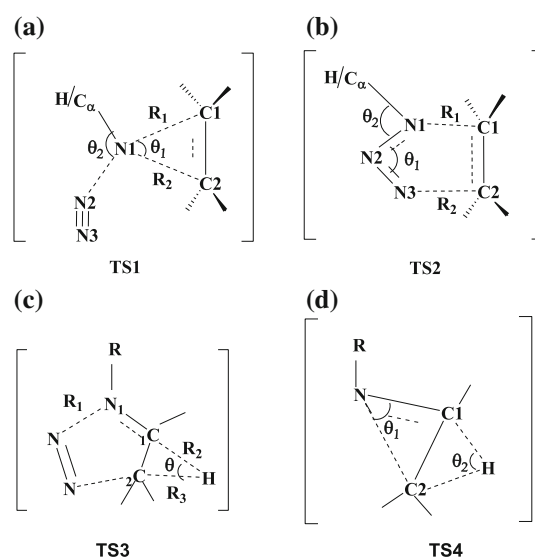


Figure 5. Geometry parameters for transition states. (a) **TS1** for concerted addition–elimination of azide to alkene, (b) **TS2** for 1,3-dipolar cycloaddition between azide and alkene, (c) **TS3** for 1,2-hydride shift in triazoline to form N-alkylimine, and (d) **TS4** for conversion of N-alkylimine to aziridine by another 1,2-hydride shift.

(d) **TS4** for conversion of N-alkylimine to the aziridine cycle by another 1,2-hydride shift (second step of second phase of Route II). These geometry parameters relate transition state geometry to the Hammond postulate and estimate position of the transition state along the reaction pathway.

3. Results and Discussion

Route I and Route II for the thermal, gas phase, uncatalyzed aziridination of alkenes by whole azide molecules are discussed as follows:

3.1 Concerted aziridination by azide (Route I)

This one-step mechanism for alkene aziridination (Figure 2) has not yet been studied before. Table 1 lists B3LYP values of the energy changes and activation barriers for this step.

The reaction energy changes ΔE_R and ΔG_R (ΔE_R always smaller in magnitude than ΔG_R) predict appreciable exothermicity (ΔE_R from -42.0 to -49.5 kcal/mol). In general, the trend for a thermodynamic facility with respect to azide substituent **R** falls in the order $\text{H} < \text{Me} < \text{Ac}$. This points to the electrophilic character of the azide reactant as it reacts with the alkene, where the electron-withdrawing acetyl substituent in the acyl azide enhances reaction facility.

Table 1. B3LYP/6-31G** values of energy parameters* for concerted aziridination of alkenes by Route I (direct action of azide $\mathbf{R-N}_3$ upon alkene *via* **TS1**; Figure 2).

Alkene	ΔE_R	ΔE^\ddagger	ΔG_R	ΔG^\ddagger
R = H				
Ethene	-42.0	38.2	-40.8	47.0
Propene A	-42.5	37.4	-40.3	47.4
Propene B	-42.2	37.7	-39.9	47.6
<i>cis</i> -2-Butene	-43.5	36.4	-41.3	46.0
<i>trans</i> -2-Butene	-43.0	36.9	-40.6	47.0
R = Me				
Ethene	-44.3	38.5	-42.1	50.1
Propene A	-44.9	38.1	-41.7	50.3
Propene B	-41.8	38.2	-38.2	52.2
<i>cis</i> -2-Butene	-46.0	41.2	-42.8	51.0
<i>trans</i> -2-Butene	-42.7	43.2	-39.4	52.2
R = Ac				
Ethene	-47.2	38.4	-46.2	49.5
Propene A	-48.1	33.2	-46.1	43.4
Propene B	-46.7	35.8	-46.0	44.2
<i>cis</i> -2-Butene	-49.5	31.5	-47.4	41.7
<i>trans</i> -2-Butene	-47.8	32.5	-45.5	42.2

*All energy terms in kcal/mol.

The activation barrier ΔE^\ddagger ranges from 31.5 to 43.2 kcal/mol, and the free energy barrier ΔG^\ddagger higher than ΔE^\ddagger by 9 to 11 kcal/mol, the correlation between the two being shown in Figure S1 (Supplementary Information). For HN_3 and AcN_3 , ΔE^\ddagger follows the order: ethene > propene > *trans*-2-butene > *cis*-2-butene. Successive methyl substitution in the alkene lowers the barrier, showing the electrophilic nature of the azide. For propene, orientation A is favored over B, due to lesser steric interactions.

Direct attack of azide on alkene is compared with the rate-determining step for Route A studied earlier, *viz.*, decomposition of azide to singlet nitrene.¹⁵ Direct attack of HN_3 gives activation barriers (36.4 to 38.2 kcal/mol) lower than the barrier for decomposition of HN_3 to NH (52.7 kcal/mol), so Route I is predicted more feasible than the rate-limiting step of Route A. For MeN_3 , the barrier for decomposition to MeN (39.4 kcal/mol) is comparable to the barriers involved in Route I (38.1 to 43.2 kcal/mol), so that these two pathways could compete. For AcN_3 , the barriers to direct attack (31.5 to 38.4 kcal/mol) are higher than the barrier for AcN_3 decomposition to AcN (28.1 kcal/mol), so that Route A is favored.

B3LYP values of geometry parameters for **TS1** (Figure 5a) are given in Table S1 (SI). The two forming N–C bond lengths R_1 and R_2 (2.199 to 2.825 Å) are shorter than the length R_3 of the breaking bond between the N1 atom and the escaping N_2 moiety (1.647

Table 2. B3LYP/6-31G** values for energy parameters* associated with 1,3-dipolar cycloaddition of azide $\mathbf{R-N}_3$ to alkene (Figure 3) *via* transition state **TS2**.

Alkene	ΔE_r	ΔE^\ddagger	ΔG_r	ΔG^\ddagger	ν_i
R = H					
Ethene	-15.4	20.6	-2.9	31.9	-452.0
Propene A	-14.4	21.9	-0.7	34.0	-444.4
Propene B	-14.4	22.3	-0.6	34.5	-450.9
<i>cis</i> -2-Butene	-14.4	23.3	-0.3	35.3	-442.9
<i>trans</i> -2-Butene	-14.0	23.4	-0.0	35.6	-437.5
R = Me					
Ethene	-18.9	19.0	-5.5	30.6	-406.6
Propene A	-17.8	20.6	-3.3	33.3	-405.9
Propene B	-16.8	20.4	-2.3	33.0	-396.8
<i>cis</i> -2-Butene	-17.5	21.5	-2.9	34.0	-390.5
<i>trans</i> -2-Butene	-16.0	22.0	-1.2	34.6	-393.8
R = Ac					
Ethene	-25.0	15.9	-12.6	27.1	-329.1
Propene A	-24.3	17.4	-10.8	29.5	-325.9
Propene B	-24.1	15.9	-10.3	28.3	-322.1
<i>cis</i> -2-Butene	-23.2	16.9	-8.9	29.3	-311.3
<i>trans</i> -2-Butene	-23.6	17.4	-9.6	29.8	-313.8

*Energy terms in kcal/mol; ν_i in cm^{-1} .

to 1.773 Å). This points to an *early* transition state for all cases. The $\langle \text{C1-N1-C2} \rangle$ angle θ_1 (30.7 to 36.0°) in **TS1** contrasted with the θ_1 values (around 60°) in the aziridine product also points to this. The $\text{C}\alpha\text{-N1-C1-C2}$ dihedral angle φ_1 (85.6 to 103.4°) indicates the **R** group is approximately perpendicular to the N1–C1–C2 plane. The N2–N1–C1–C2 dihedral φ_2 values show that the dinitrogen moiety has its N2 atom within the N1–C1–C2 plane for the HN_3 cases, but out of the plane for the MeN_3 and AcN_3 cases. The prediction of early character for **TS1** accords well with Hammond's postulate for these exothermic reactions.

3.2 Two-phase aziridination by azide (Route II)

The two phases for Route II (Figures 3 and 4) are (a) 1,3-dipolar cycloaddition between azide and alkene *via* transition state **TS2** to form a triazoline, and (b) decomposition of triazoline to yield aziridine in two steps – triazoline ring cleavage *via* **TS3**, followed by cyclization of the intermediate *via* **TS4**.

3.2a *Phase (a)*: Table 2 presents values of the energy changes ΔE_r and ΔG_r with the activation barriers ΔE^\ddagger and ΔG^\ddagger for 1,3-dipolar cycloaddition, and ν_i , the imaginary frequency involved. The reaction energy change is modest (ΔE_r from -14.0 to -25.0 kcal/mol, and ΔG_r from -0.0 to -12.6 kcal/mol). Thermodynamic facility falls in the order $\text{Ac} > \text{Me} > \text{H}$, indicating the acetyl substituent facilitates this step. Successive methyl

Table 3. B3LYP/6-31G** values of energy parameters* for two-step decomposition of the triazoline intermediate to yield aziridine and dinitrogen *via* **TS3** and **TS4** (Figure 4).

Alkene	$\Delta E_r(1)$	$\Delta E^\ddagger(1)$	$\Delta G_r(1)$	$\Delta G^\ddagger(1)$	$\Delta E_r(2)$	$\Delta E^\ddagger(2)$	$\Delta G_r(2)$	$\Delta G^\ddagger(2)$
R = H								
Ethene	-49.0	33.9	-61.1	32.7	22.4	88.8	23.2	89.0
Propene A	-51.8	31.6	-64.3	30.2	17.8	85.9	18.7	86.4
Propene B	-46.1	33.2	-58.4	32.1	23.7	89.1	24.8	90.2
<i>cis</i> -2-Butene	-48.3	31.1	-61.5	29.3	19.2	82.6	20.6	83.5
<i>trans</i> -2-Butene	-48.5	31.8	-61.3	30.6	19.4	81.3	20.6	82.5
R = Me								
Ethene	-49.0	33.8	-61.2	32.4	23.6	86.7	24.7	86.8
Propene A	-49.4	31.1	-63.2	29.3	18.5	78.3	19.7	78.7
Propene B	-45.7	34.8	-58.1	33.3	21.3	87.1	23.9	89.3
<i>cis</i> -2-Butene	-45.4	33.9	-58.8	32.0	16.9	79.3	18.9	80.6
<i>trans</i> -2-Butene	-46.5	33.3	-59.7	31.7	19.8	79.2	21.6	80.5
R = Ac								
Ethene	-42.1	31.1	-54.2	29.7	19.9	82.8	20.6	86.8
Propene A	-38.3	27.1	-50.6	25.3	14.4	71.4	15.5	72.6
Propene B	-38.1	30.5	-49.4	29.1	15.2	72.3	16.1	73.4
<i>cis</i> -2-Butene	-41.5	27.6	-54.9	25.5	15.2	75.2	16.4	80.7
<i>trans</i> -2-Butene	-45.9	32.4	-58.8	30.7	18.1	77.9	19.4	79.5

*All energy terms in kcal/mol.

substitution on the alkene reduces reaction facility, attributable to steric effects. The reaction energy change ΔE_r for MeN_3 addition to ethene (-18.9 kcal/mol) may be compared with other estimates²² (in kcal/mol) as follows: AM1 (-25.2); B3LYP/6-311++G** (-21.7); HF/6-31G* (-32.7); MP2/6-31G* (-26.1); B3LYP/6-31G* (-27.9); MP2/6-311++G** (-25.4); B3LYP/6-31G**//AM1 (-25.8); QCISD/6-31G* (-31.8). In general, our ΔE_r value is on the smaller side.

The cycloaddition barriers ΔE^\ddagger (15.9 to 23.4 kcal/mol) are lower by 11–12 kcal/mol than the free energy barriers ΔG^\ddagger . The barriers follow the order H > Me > Ac. The kinetic facility order is the same as that for the thermodynamic facility. The acetyl substituent enhances kinetic facility by stabilizing the transition state **TS1** through resonance delocalization.

Successive methyl substitution on the alkene increases the barrier, diminishing kinetic as well as the thermodynamic facility. Our ΔE^\ddagger value of 19.0 kcal/mol for MeN_3 cycloaddition to ethene compares with other estimates²² (in kcal/mol) as follows: AM1 (36.4); B3LYP/6-311++G** (19.7); HF/6-31G* (22.5); MP2/6-31G* (17.8); B3LYP/6-31G* (15.9); MP2/6-311++G** (11.2); B3LYP/6-31G**//AM1 (27.8) and QCISD/6-31G* (24.7). Our estimate is lower than the QCISD estimate (24.7 kcal/mol), but higher than the MP2/6-311++G** estimate. 1,3-Dipolar cycloaddition to alkynes leads to barriers lower than for alkenes, where our value for MeN_3 addition to ethyne (15.0 kcal/mol) is comparable with the low B3LYP values of 11.4

and 12.8 kcal/mol [6-311+G(d,p) and 6-311+G(3df,2p) basis sets respectively] for [2+3] cycloaddition between cyclooctyne and phenyl azide.²⁸

B3LYP/6-31G** values of geometry parameters* for **TS2** defined in Figure 5b are given in Table S2 (SI). The long forming C1–N and C2–N bond lengths R_1 and R_2 (2.156 to 2.281 Å) suggest early transition states in line with the exothermicity of these reactions. The N1–N2–N3 angle θ_1 (134.5 to 137.6°) suggests the N2 atom is between *sp* and *sp*². The N2–N1–C α /H angle θ_2 point to an *sp*³ N1 atom for the HN_3 cases, but an *sp*² N1 atom for the MeN_3 and AcN_3 cases. The [H/C α –N1–N3–N2] dihedral angle φ_1 and the [H/C α –C1–C2–N3] dihedral angle φ_2 (132.8 to 159.1°) predict the H and Me groups are out of the C1–C2–N3–N2–N1 ring plane. φ_1 and φ_2 values close to 180° predict the acetyl group is within this ring plane since the Ac group resonates with the ring pi electrons (a stabilizing feature).

3.2b Phase (b): The second phase of 1,3-dipolar cycloaddition of MeN_3 to C_{60} with the elimination of N_2 from the triazoline intermediate to yield aziridine had been studied by semi-empirical and DFT methods earlier.³⁰ Since our alkene systems have no supporting framework like that present in C_{60} , there is no scope to treat thermal N_2 elimination from the triazoline intermediate in a concerted fashion. Our attempts to force this reaction as a concerted adiabatic process did not lead to any transition state. Hence our proposal for a two-step process *via* two successive 1,2-hydride shifts

Table 4. B3LYP/6-31G** values* for the highest point along each of the four routes for thermal uncatalyzed aziridination of 4 alkenes by 3 azides RN_3 .

Reactants	Route A	Route B	Route I	Route II
HN_3				
Ethene	52.7	52.7	38.2	20.6
Propene	52.7	52.7	37.4	21.9
<i>cis</i> -2-Butene	52.7	52.7	36.4	23.3
<i>trans</i> -2-Butene	52.7	52.7	36.9	23.4
MeN_3				
Ethene	39.4	39.4	38.5	19.0
Propene	39.4	39.4	38.2	20.6
<i>cis</i> -2-Butene	39.4	39.4	41.2	21.5
<i>trans</i> -2-Butene	39.4	39.4	43.2	22.0
AcN_3				
Ethene	28.1	28.1	38.4	15.9
Propene	28.1	28.1	35.8	17.4
<i>cis</i> -2-Butene	28.1	28.1	31.5	16.9
<i>trans</i> -2-Butene	28.1	28.1	32.5	17.4

*All energy terms in kcal/mol.

(Figure 4) involving an N-alkylimine intermediate.³⁰ Decomposition of triazoline to aziridine and N_2 may, however, be concerted under photochemical conditions.⁴⁰

Values of the reaction energy changes $\Delta E_r(1)$ and $\Delta G_r(1)$ and the barriers $\Delta E^\ddagger(1)$ and $\Delta G^\ddagger(1)$ are given in Table 3 for the first step of phase (b) of Route II. Rearrangement of the triazoline is exothermic ($\Delta E_r = -38.1$ to -51.8 kcal/mol; $\Delta G_r = -49.4$ to -64.3 kcal/mol), being less pronounced for the AcN_3 cases due to stabilization of the triazoline intermediate by the acetyl group through resonance. The propene A case is favored thermodynamically and kinetically over the propene B case due to steric effects.

Geometry parameters for **TS3** (Figure 5c) for triazoline decomposition are given in Table S3 (SI). R_1 and R_2 represent lengths of the cleaving N1–N and C1–H* bonds (H* is the migrating hydride atom), and R_3 represents the length of the forming C2–H* bond. Since this first step is exothermic, **TS3** is expected to be “early”. Now the N1–N bond lengths R_1 do not point to an early transition state. However, the cleaving C1–H* bond length R_2 (1.110 to 1.160 Å) is short, while the forming C2–H bond length R_3 (1.710 to 1.958 Å) is long. It is the C–H bonds involved in 1,2-hydride shift which determine the “early” character of **TS3**, rather than loss of the N_2 moiety. The acute C1–H*–C2 angle θ (47.9 to 58.0°) also shows early character.

Transition state **TS4** for the second step of phase (b) has geometry parameters given in Table S4 (SI). The 1,2-hydride shift cum cyclization is endothermic, so transition state **TS4** is expected to be ‘late.’ The forming N–C bond length R_1 between the apical N-atom

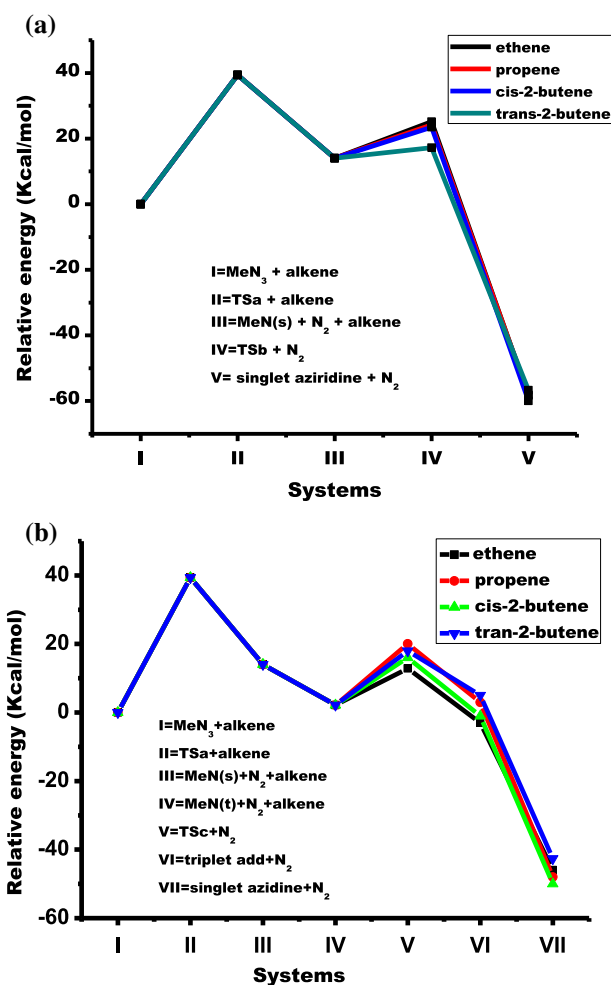


Figure 6. Energy profiles for thermal gas-phase aziridination of alkenes by methyl azide, as given by (a) Route A, and (b) Route B, both involving the discrete nitrene intermediate (results of earlier work¹⁵ using the B3LYP/6-31G** method). (a) Route A (b) Route B.

and the C2 atom (2.307 to 2.426 Å) is longer than this length (~ 1.47 Å) in the aziridine product, which indicates early character. The acute C1–N–C2 bond angle θ_1 (31.7 to 37.2°) compared to the $\sim 60^\circ$ values in the aziridine product also indicates the same. So, the cyclization process does not contribute to the late character. However, the forming C1–H* bond length R_2 is short (1.113 to 1.167 Å) while the breaking C2–H* bond length R_3 is long (1.769 to 2.092 Å), pointing to the late character for **TS4**. The C1–H*–C2 bond angle θ_2 (41.1 to 55.3°) is also less acute. It is thus the 1,2-hydride migration process which determines the late character of **TS4**, not the cyclization process.

3.3 Comparison of four aziridination mechanisms

This work, together with an earlier one, delineates four distinct mechanisms for gas phase aziridination of

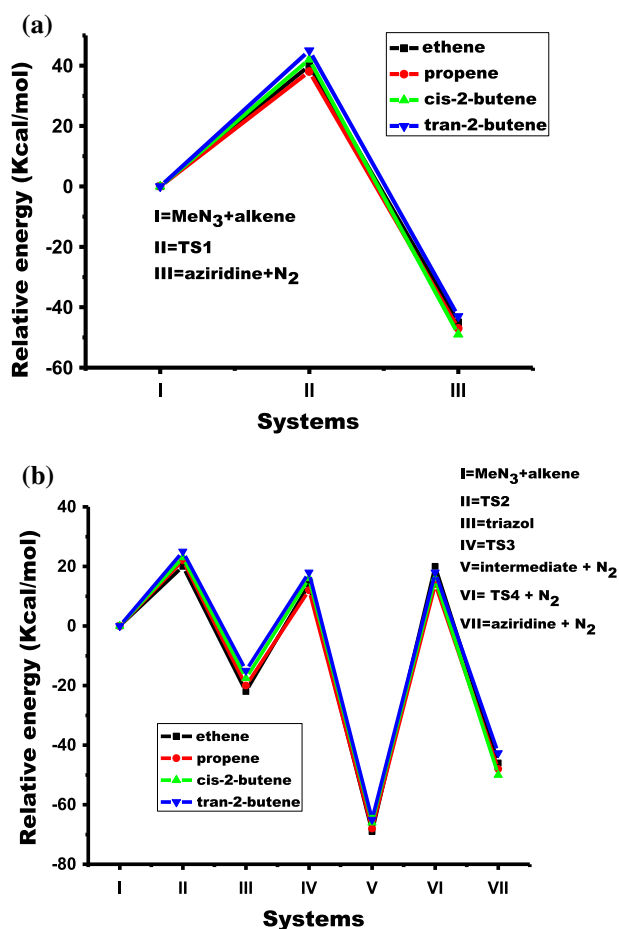


Figure 7. Energy profiles for thermal gas-phase aziridination of alkenes by methyl azide, as given by (a) Route I, and (b) Route II, both involving the whole azide reactant molecule (results of this work using B3LYP/6-31G** method). (a) Route I (b) Route II.

alkenes by azides – Route I and Route II (involving whole azide molecules), and Route A and Route B of the earlier study¹⁵ (involving discrete nitrene intermediates). We compare the energy profiles of all four pathways to predict the most favorable. Table 4 lists the energy level of the highest point along each route for the three azide reactants RN_3 ($\text{R} = \text{H}, \text{Me}, \text{Ac}$) reacting with the four alkene substrates.

Figure 6a depicts the energy profiles for Route A involving singlet nitrene generation *via* transition state **TSa** followed by singlet nitrene addition to alkene *via* transition state **TSb**. Figure 6b shows the energy profiles for multi-step Route B involving azide decomposition to singlet nitrene, singlet to triplet conversion, triplet nitrene addition to alkene *via* **TSc**, and triplet to singlet conversion to the aziridine product. Figures 6a and 6b portray only the cases for MeN_3 . For both Route A and Route B, the highest point concerns only the azide reactant decomposition to the singlet nitrene RN , being the same for all alkene substrates.

Figure 7a portrays energy profiles for Route I, while Figure 7b gives energy profiles for Route II, depicting the cases for methyl azide. The highest point for Route I is **TS1** for whole azide concerted addition to alkene forming aziridine. For Route II, involving transition states **TS2**, **TS3** and **TS4**, the highest point is **TS2** for 1,3-dipolar cycloaddition of azide to alkene.

We infer from Table 4 that gas phase thermal aziridination of alkenes by azides is most feasible by the multi-step Route II involving initial 1,3-dipolar cycloaddition of the whole azide to alkene. This entails an energy requirement of 15.9 to 23.4 kcal/mol. We thus conclude that gas phase aziridination of alkenes under thermal conditions would most easily proceed by a mechanism involving prior 1,3-dipolar cycloaddition between azide and alkene.

4. Conclusions

This DFT B3LYP/6-31G** study on azide addition to alkenes forming aziridines by two distinct mechanisms (Routes I and II) leads to the following conclusions:

1. Route I by direct concerted addition–elimination of azide to alkene (studied here for the first time) involves appreciable barriers, being assisted by methyl substitution on the alkene, showing the azide to have electrophilic character.
2. The first step of Route II (1,3-dipolar cycloaddition of azide to alkene) yields appreciable barriers (15.9 to 23.4 kcal/mol) and the facility order $\text{Ac} > \text{Me} > \text{H}$ with respect to azide substituent R , but is not assisted by methyl substitution on the alkene.
3. The second phase of Route II involves an N-alkylimine intermediate which cyclizes to the aziridine product by two successive hydride shifts. It is these hydride shifts that contribute significantly to the late character of the transition states involved.
4. Concerted decomposition of the 1,3-dipolar cycloaddition product is exothermic with appreciable barriers (27.1 to 33.9 kcal/mol) and assisted by methyl substitution on the initial alkene reactant.
5. The endothermic final step of Route II (cyclization of N-alkylimine to aziridine) involves very high barriers, accompanied by appreciable net energy lowering for the second phase of Route II.
6. The geometries of the various transition states for the various concerted steps are characterized as ‘early’ or ‘late’ in good accord with Hammond’s postulate.
7. Of all four routes examined for aziridination of alkenes by azides, Route II involving 1,3-dipolar cycloaddition between azide and alkene is predicted as most favorable.

Supplementary Information (SI)

Supplementary Information is available at www.ias.ac.in/chemsci.

Acknowledgements

S. P. D. thanks the University Grants Commission for financial assistance through the UGC Research Fellowship for Meritorious Students.

References

1. Padwa A and Murphree S S 2006 Epoxides and aziridines – a mini review *ARKIVOC* **3** 6
2. Hennessy J 2014 Aziridine synthesis *Nature Chem.* **6** 168
3. Bellavia-Lund C and Wudl F 1997 Synthesis of [70] aza-fulleroids: Investigations of azide addition to C₇₀ *J. Am. Chem. Soc.* **119** 943
4. Averdung J, Luftmann H, Mattay J, Claus K and Abraham W 1995 Synthesis of 1,2-(2,3-dihydro-1H-azirino)-[60]fullerene, the parent fulleroaziridine *Tetrahedron Lett.* **36** 2957
5. Scriven E F V and Turnbull C K 1988 Azides: Their preparation and synthetic uses *Chem. Rev.* **88** 297
6. Carmen Gil S B, Knepper K and Zimmermann V 2005 Organic azides: An exploding diversity of a unique class of compounds *Angew. Chem. Int. Ed.* **44** 5188
7. Pellisier H 2014 Recent developments in asymmetric aziridination *Adv. Synth. Catal.* **356** 1899
8. Osborn H M I and Sweeney J 1997 The asymmetric synthesis of aziridines *Tetrahedron Asymmetry* **11** 1693
9. Xue Z, Louisa V M D, Weeks J H, Whittlesey B R and Mayer M F 2010 Asymmetric aziridination of N-tert-butanesulfinyl imines with phenyldiazomethane via sulfur ylides *ARKIVOC* **7** 65
10. Janardanan D and Sunoj R B 2008 Enantio- and diastereoselectivities in chiral sulfur ylide promoted asymmetric aziridination reactions *J. Org. Chem.* **73** 8163
11. Aggarwal V K, Alonso E, Fang G, Ferrara M, Hynd G and Porcelloni M 2001 Application of chiral sulfides to catalytic asymmetric aziridination and cyclopropanation with in situ generation of the diazo compound *Angew. Chemie Int. Ed.* **40** 1433
12. Li Z, Conser K R and Jacobsen E N 1993 Asymmetric alkene aziridination with readily available chiral diimine-based catalysts *J. Am. Chem. Soc.* **115** 5326
13. Li Z, Quan R W and Jacobsen E N 1995 Mechanism of the (diimine)copper-catalyzed asymmetric aziridination of alkenes. Nitrene transfer via ligand-accelerated catalysis *J. Am. Chem. Soc.* **117** 5889
14. Wu H, Xu L-W, Xia C-G, Ge J and Yang L 2005 Convenient metal-free aziridination of alkenes with chloramine-T using tetrabutylammonium iodide in water *Synth. Comm.* **39** 1413
15. Devi S P, T Salam and Duncan Lyngdoh R H 2016 Uncatalyzed thermal gas phase aziridination of alkenes by organic azides. Part I: Mechanisms with discrete nitrene species *J. Chem. Sci.* **128** 681
16. Padwa A and Pearson W H (Eds.) 2002 Synthetic applications of 1,3-dipolar cycloaddition chemistry toward heterocycles and natural products In *The Chemistry of Heterocyclic Compounds* Vol. 59 (New York: Wiley)
17. Sha C K and Mohanakrishnan A K 2002 Azides in synthetic applications of 1,3-dipolar cycloaddition chemistry towards heterocycles and natural products Vol 59 A Padwa and W H Pearson (Eds.) (New York: Wiley)
18. Huisgen R 1961 Centenary lecture – 1,3-dipolar cycloadditions *Proc. Chem. Soc. London* 357
19. Meldal M and Tornøe C W 2008 Cu-catalyzed azide-alkyne cycloaddition *Chem. Rev.* **108** 2952
20. Kolb H C, Finn M G and Sharpless K B 2001 Click chemistry: diverse chemical function from a few good reactions *Angew. Chem. Int. Ed.* **40** 2004
21. Baskin J M, Prescher J A, Laughlin S T, Agard N J, Chang P V, Miller I A, Lo A, Codelli J A and Bertozzi C R 2007 Copper-free click chemistry for dynamic *in vivo* imaging *Proc. Natl. Acad. Sci. USA* **104** 16793
22. Ess D H and Houk K N 2008 Theory of 1,3-dipolar cycloadditions: Distortion/interaction and frontier molecular orbital models *J. Am. Chem. Soc.* **130** 10187
23. Chen X F, Yang K and Han K L 2009 Theoretical study of 1,3-dipolar cycloaddition of hydrazoic acid to substituted ynamines *Chin. J. Chem. Phys.* **22** 43
24. Schoenebeck F, Ess D H, Jones G O and Houk K N 2009 Reactivity and regioselectivity in 1,3-dipolar cycloadditions of azides to strained alkynes and alkenes: A computational study *J. Am. Chem. Soc.* **131** 8121
25. Karmakar S and Datta A 2015 Metal-free azide-alkyne click reaction: role of substituents and heavy atom tunneling *J. Phys. Chem. B* **119** 11540
26. Washington I and Houk K N 2003 Strategies for the design of organic aziridination reagents and catalysts: Transition structures for alkene aziridinations by NH transfer *J. Org. Chem.* **68** 6497
27. Almahy H A and Elhassan E 2013 Spectroscopic study of 1,3-dipolar cycloaddition reaction of benzyl azide and acrylic acid *Int. J. Chem. Sci.* **11** 1
28. Bach R D 2009 Ring strain energy in the cyclooctyl system. The effect of strain energy on [3+2] cycloaddition reactions with azides *J. Am. Chem. Soc.* **131** 5233
29. Zeghada A, Bentabed-Ababsa G, Derdour A, Abdelmounim S, Domingo L R, S'aez J A, Roisnel T, Nassare E and Mongin F 2011 A combined experimental and theoretical study of the thermal cycloaddition of aryl azides with activated alkenes *Org. Biomol. Chem.* **9** 4295
30. Cases M, Duran M, Mestres J, Martin N and Sola M 2001 Mechanism of the addition reaction of alkyl azides to [60]fullerene and the subsequent N₂ extrusion to form monoimino-[60]fullerenes *J. Org. Chem.* **66** 433
31. Janardanan D and Sunoj R B 2007 Computational investigations on the general reaction profile and diastereoselectivity on sulfur ylide promoted aziridination *Chem. Eur. J.* **13** 4805
32. Rajeev R and Sunoj R B 2011 Mechanism and electronic effects in nitrogen ylide-promoted asymmetric aziridination reaction *Org. Biomol. Chem.* **9** 2123

33. Jaccob M and Venuvanalingam P 2011 Computational insights into the roles of steric and electrostatic interactions in arsenic ylide mediated aziridination reactions *Eur. J. Org. Chem.* 3458
34. Kalaiselvan A and Venuvanalingam P 2007 Ring opening of boriranes vis-à-vis aziridines: An ab initio and DFT probe on the mechanisms *Int. J. Quantum Chem.* **107** 1590
35. Lee C, Yang W and Parr R G 1988 Development of the Colle-Salvetti correlation-energy formula into a functional of the electron density *Phys. Rev. B* **37** 785
36. Becke A D 1993 A new mixing of Hartree-Fock and local density-functional theories *J. Chem. Phys.* **98** 1372
37. Scott A P and Radom L 1996 Harmonic vibrational frequencies: An evaluation of Hartree-Fock, Møller-Plesset, quadratic configuration interaction, density functional theory and semiempirical scale factors *J. Phys. Chem.* **100** 16502
38. Frisch M J, Trucks G W, Schlegel H B, Scuseria G E, Robb M A, Cheeseman J R, Scalmani G, Barone V, Mennucci B, Petersson G A, Nakatsuji H, Caricato M, Li X, Hratchian H P, Izmaylov A F, Bloino J, Zheng G, Sonnenberg J L, Hada M, Ehara M, Toyota K, Fukuda R, Hasegawa J, Ishida M, Nakajima T, Honda Y, Kitao O, Nakai H, Vreven T, Montgomery J A, Peralta J E, Ogliaro F, Bearpark M, Heyd J J, Brothers E, Kudin K N, Staroverov V N, Keith T, Kobayashi R, Normand J, Raghavachari K, Rendell A, Burant J C, Iyengar S S, Tomasi J, Cossi M, Rega N, Millam J M, Klene M, Knox J E, Cross J B, Bakken V, Adamo C, Jaramillo J, Gomperts R, Stratmann R E, Yazyev O, Austin A J R, Pomelli C C, Ochterski J W, Martin R L, Morokuma K, Zakrzewski V G, Voth G A, Salvador P, Dannenberg J J, Dapprich S, Daniels A D, Farkas O, Foresman J B, Ortiz J V, Cioslowski J, Fox D J, Gaussian, Inc., Wallingford CT, Gaussian 09, Revision C.01, **2010**
39. Hammond G S 1955 A correlation of reaction rates *J. Am. Chem. Soc.* **77** 334
40. Burgess E M, Carithers R and McCullagh L 1968 Photochemical decomposition of 1H-1,2,3-triazole derivatives *J. Am. Chem. Soc.* **90** 1923